ELSEVIER

Dyes and Pigments 43 (1999) 95–108

DYES and PIGMENTS

Degradation of commercial reactive dyestuffs by heterogenous and homogenous advanced oxidation processes: a comparative study

I. Arslan, I. Akmehmet Balcioğlu*

Institute of Environmental Sciences, Bogaziçi University, 80815 Bebek, Istanbul, Turkey

Abstract

Advanced oxidation of the commercially available reactive dyestuffs Remazol Black B and Remazol Turquoise Blue G 133 in aqueous solution with TiO_2-mediated photocatalytic and photoinduced and dark Fenton/Fenton-like reactions has been studied. Initial decolourization rates, effectiveness in removal of $UV_{254\ nm}$, COD as well as TOC were compared and evaluated. It was found that all advanced oxidation systems were capable of completely decolourizing the azo dye Remazol Black in feasible treatment times and at concentrations typically found in dyehouse effluents, whereas COD and TOC removal efficiencies ranged between 77–98% and 51–86%, respectively. Photo-Fenton's oxidation gave the best decolourization reaction, which proceeded 20 times faster than TiO_2-mediated photocatalytic oxidation. Moreover, photocatalytical treatment of Remazol Black followed the empirical Langmuir–Hinshelwood kinetics in the concentration range 25–100 mg/l. However, none of the advanced oxidation systems was effective in the degradation of the copper phthalocyanine dye Remazol Turquoise Blue for which colour and COD removal was mainly attributable to adsorption on the photocatalyst surface or the coagulating effect of iron applied in the homogenous advanced oxidation reactions.

Keywords: Photocatalytic degradation; TiO_2; Fenton's reagent; Photo-Fenton reaction; Advanced oxidation processes; Reactive Remazol dyes

1. Introduction

Effluents from the dyeing and finishing processes in the textile industry are known to contain strong colour, high amounts of surfactants, dissolved solids, fluctuating temperature, high pH and possibly heavy metals (e.g. Cu, Cr, Ni) [1]. From the environmental point of view, particularly the removal of synthetic dyes is of great concern, since they or their degradation products might be of toxic nature and consequently their treatment cannot depend on biodegradation alone [2,3]. Hence, decolourization of dyehouse effluents has become the integral part of textile wastewater treatment.

At present, so called "integrated processes" involving various combinations of biological, physical and chemical treatment methods are used for decolourization of textile effluents but with limited success [4,5]. Our preliminary experiments

* Corresponding author.
E-mail address: balciogl@boun.edu.tr (I.A. Balcioğlu)

0143-7208/99/$ - see front matter
PII: S0143-7208(99)00048-0

have shown that colour removal using aluminium sulphate for coagulation of real textile effluents at the 8–10 pH range did not exceed 50% [6].

An alternative to traditional methods are Advanced Oxidation Processes (AOPs) based on the generation of very reactive species such as hydroxyl radicals ($OH^{\bullet}$) that oxidize a broad range of organic pollutants quickly and non-selectively [7]. Homogenous (Fenton's reagent, light-assisted Fenton's oxidation, H_2O_2/UV treatment, ozonation at high pH etc.) and heterogenous (semiconductor-mediated photocatalysis) advanced oxidation systems have been thoroughly and comparatively evaluated for a variety of organic compounds and wastewaters in the past. Also several investigations have demonstrated that AOPs are effectively removing colour and partially organic content of dyestuffs [8–11]. Other investigations have focused on the photoinduced degradation of several dyestuffs by TiO_2 photocatalysis and photo-Fenton's reaction which are applicable under solar and near-UV irradiation [12–17]. However, a comparative study evaluating homogenous with heterogenous treatment systems in terms of reaction kinetics, oxidation rates and efficiencies is substantially missing from the literature.

The greater demand for brilliant hues and a greater prevalence of short run lots have increased the demand for reactive dyes worldwide. Unfortunately, the major limitation of their success is that as much as 50% of total cost of reactive dyeing must be attributed to the washing-off stages and treatment of the resulting effluent [18].

Among the reactive dyes, Remazol Black B is one of the oldest and has a very large consumption rate in textile dyeing processes. Reactive copper phthalocyanine dyes like Remazol Turquoise Blue G133 are preferred to direct dyes due to their brilliant hue, excellent light and wet fastness wherever high quality turquoises, greens and blues are desired. Both dyes appear in the washwater in their hydrolyzed or unfixed form at levels that depend upon the degree of fixation on the fabric and the type of dyeing process applied, and end up in the dyehouse effluent [18].

In the present investigation, TiO_2-mediated photocatalytic oxidation (PCO) and Fenton/Fenton-like reactions were applied to the reactive copper phthalocyanine dye Remazol Turquoise Blue G133 and the reactive azo dye Remazol Black B in aqueous solutions. These dyes were selected as typical dyestuffs to represent reactive dye groups with relatively higher consumption rates in the cotton dyeing process. Experiments were conducted at dye concentrations typically present in dyehouse effluents. Treatment performance of the two oxidation systems were compared and evaluated in terms of widely used environmental parameters such as TOC, COD, UV-visible spectrophotometry and initial decolourization rates.

2. Materials and methods

2.1. Materials

The commercially available reactive dyestuffs Remazol Black B and Remazol Turquoise Blue G133 were obtained from Dystar Hoechst Corporation. The TiO_2 used in the photocatalytical runs was Degussa P-25 consisting of mainly anatase crystalline form, a surface area of approximately 50 m^2/g and a mean diameter of 30 nm. H_2O_2 (30% w/w) was supplied by Merck. All other reagents were reagent grade.

Distilled deionized water was used to prepare of dye solutions and solutions of ferric nitrate and ferrous sulphate for the Fenton and Fenton-like oxidation runs. The characterization of the dyestuffs is presented in Table 1 for 75 mg/l dye solutions. The molecular structure of Reactive Black 5 is exactly known [18], whereas that of Reactive Blue 21 is not known.

2.2. Photoreactor and light source

A 20 W black light fluorescent (BLF) lamp (General Electric) was positioned within the center of a 1000 cm^3-borosilicate glass annular photoreactor operating at batch mode. The absorbed fluence rate in the photoreactor was found by potassium ferrioxalate actinometry as 1.30×10^{-5} Einsteins/(m^2.s). A detailed description of the photoreactor has been presented elsewhere [6]. The reactions were carried out at room temperature

Table 1
Characterization of the dyestuffs

Parameter	Turquoise Blue G133	Remazol Black B
Class	Copper phthalocyanine	Diazo
Colour index name	Reactive Blue 21	Reactive Black 5
Reactive group	Sulphatoethylsulphone	Sulphatoethylsulphone
pH	5.12	5.54
COD (mg/l)	46.93	46.38
TOC (mg/l)	18.62	12.72
λ_{max} (nm, visible-UV region)[a]	662[b], 626, 342	597, 391
Molecular weight (g/mol)	576.10	991.80
BOD_5	Not detectable	Not detectable
Purity (%)	Not specified	80–85

[a] Monitored in 1 cm quartz cells at their natural pH.
[b] This peak disappeared below pH = 4.

(18–20°C). Aliquots of treated samples were taken periodically from the reactor up to 2 h and filtered through 0.45 μm Millipore membranes prior to immediate analysis.

2.3. Analytical measurements

A Shimadzu Model UV-160 double beam spectrophotometer was employed to record absorbance in the UV-visible region with 1 cm quartz cells. TOC was measured using a TOC analyzer-450 (Carlo-Erba; Fisons Instruments). All other analysis were made according to standard methods.

Dye concentrations at identical conditions were determined with the spectrophotometer by preparation of a calibration curve at different pH values. The decrease in the absorbance peaks (626 nm for Remazol Turquoise Blue G 133 and 597 nm for Remazol Black B) in the visible region was directly proportional to the reduction in dye concentration.

2.4. Experimental procedure

2.4.1. Dark adsorption tests

To assess adsorption properties of the dye, 100 ml, 75 mg/l solutions of both dyestuffs were treated for 24 h at five concentrations of the photocatalyst ranging from 0.25 to 2 g/l at pH 4 and room temperature, in a mechanical shaker. Furthermore, to permit the adsorption/desorption equilibrium to be reached with 1 g/l TiO_2, 75 mg/l dye solutions were treated in the reactor described above for 2 h at pH 4 without illumination. Prior to all photocatalytic runs, different concentrations of dye solutions were equilibrated for this predetermined time period in the absence of light until a steady state dye concentration was achieved.

2.4.2. Photocatalytical experiments

Solutions containing the dyes at concentrations varying from 25 to 150 mg/l were prepared at pH 4, which was chosen as the optimum pH for decolourization by photocatalytic oxidation. The target pH was achieved using 1 M HCl. To 1 l of the prepared dye solutions TiO_2 (1 g) was added and mixed for 10 min in a sonicator to give a uniform suspension. Then the solutions were placed into the photoreactor and irradated. Sampling was carried out for 2 h at regular time intervals.

2.4.3. Fenton and Fenton-like reactions

Dark and light reactions were carried out in the same reactor described above. Ferrous and ferric ions were introduced as ferrous sulphate and ferric nitrate solutions (5×10^{-4} M) respectively. Subsequently, the pH of the dye solution was adjusted to 3 and the reaction solution was placed into the photoreactor. Finally, 5×10^{-3} M H_2O_2 was added to give a Fe^{n+}:H_2O_2 molar ratio of 1:10 in the final reaction mixture. Oxidant dosages and reaction

pH were chosen on the basis of previous optimization studies [6,19]. Spectrophotometric measurements were conducted only in the visible region for experiments involving iron salts, due to interference of ferric/ferrous ion with spectrophotometry in the UV/near-UV region.

Due to interferences of H_2O_2 with the analytical measurements, MnO_2 powder was added to destroy residual H_2O_2 in the treated solution. Since during Fe^{n+}/H_2O_2 reactions decomposition of Remazol Black B occurred almost immediately before excess H_2O_2 could be destroyed and Remazol Turquoise Blue G 133 was adsorbed on MnO_2, spectrophotometric measurements were done directly after sampling for homogenous AOPs.

3. Results and discussion

3.1. Absorption spectra of the dyes

Both dyes absorb strongly in the visible and UV region with absorption maxima at 597 and 391 nm for Remazol Black B and 662, 626 and 342 nm for Remazol Turquoise Blue G 133. The optical spectrum for Remazol Turquoise Blue G 133 remains invariant in the pH range 4–10, but significantly changes below pH < 4 (disappearance of the 662 nm absorption band).

3.2. Dark adsorption studies

Data obtained from the adsorption experiments were fitted to the Langmuir equation for both Remazol dyes. The dimensionless separation factor (R_L) indicated the shape of the Langmuir isotherm to be either favourable ($0 < R_L < 1$), unfavourable ($R_L > 1$), linear ($R_L = 1$), or irreversible ($R_L = 0$) [20,21]. According to this factor, dark adsorption on TiO_2 is favourable for both Remazol dyes. Table 2 contains the Langmuir parameters y_m, which is the amount of dye adsorbed corresponding to monolayer coverage (K_L), the Langmuir constant, and R_L, the separation factor. From the data it is obvious that adsorption on TiO_2 is fairly good for both dyes.

Adsorption studies were also conducted at neutral and basic pH values. It was observed that increasing the pH resulted in significant decrease in adsorption on TiO_2. Both dyes are anionic in aqueous solution. This phenomena explains their adsorption on positively charged TiO_2 at pH < 6.8.

Table 2
Langmuir constants for Remazol Black B and Remazol Turquoise Blue G 133 and their corresponding regression coefficients

Constant	Remazol Black B	Remazol Turquoise Blue G133
y_m (mg/g)	26.04	118.55
K_L (mg/l)	0.42	3.42
R_L[a]	0.03	3.89×10^{-3}
R^2	1.00	0.99

[a] $R_L = (1 + K_L \times C_o)$; C_o is the highest initial dye concentration.

Dark adsorption studies conducted for 2 h in the photoreactor confirmed that full equilibrated adsorption was attained after 80 min for the azo dye and 20 min for the copper complex dye. Dye solutions were preequilibrated for these time intervals prior to photocatalytic reactions conducted in the photoreactor.

3.3. Photocatalytic degradation of dyes

The photocatalytic decolourization of Remazol Black B was examined in the 25–150 mg/l initial concentration range (Fig. 1).

Control experiments carried out for 75 mg/l Remazol Black B in the absence of TiO_2 and light indicated 6 and 24% decolourization, respectively, following a 2 h reaction period. Individually, photocatalytic decolourization rates at different initial dye concentrations followed first order kinetics. By increasing the initial dye concentration up to 100 mg/l, the initial photocatalytic decolourization rate was accelerated from 3.33 1/(m.min) to 4.76 1/(m.min). However, above this concentration the decolourization rate abruptly decreased. This trend for Remazol Black B can be described by the Langmuir–Hinshelwood expression, where at high concentrations the reaction rate is zero order with respect to dye concentration and, in contrast, for concentrations under a certain value (in the present study under 150 mg/l), the reaction rate will appear to be first order

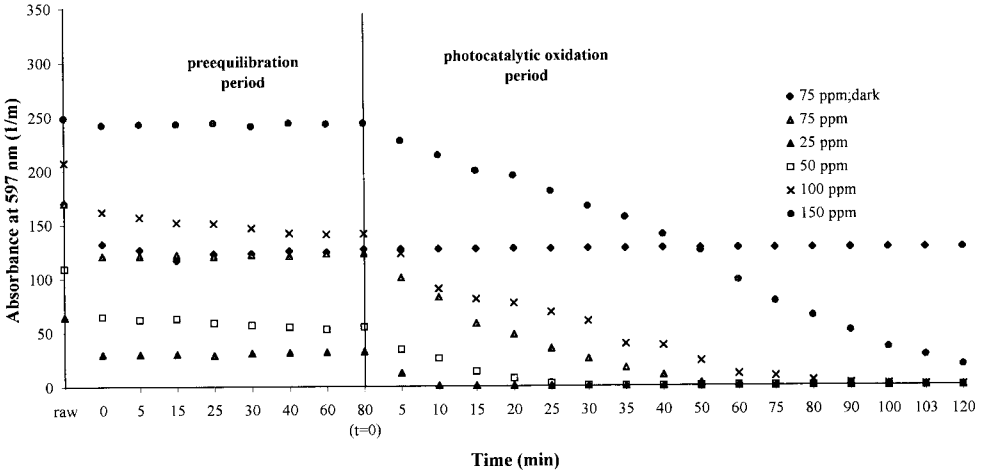

Fig. 1. Photocatalytic decolourization of Remazol Black B at various initial concentrations.

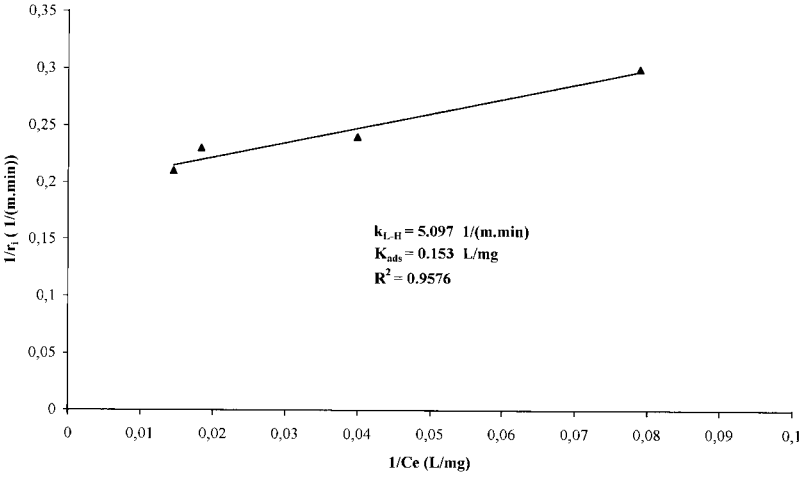

Fig. 2. Langmuir–Hinshelwood plot for Remazol Black B.

with respect to dye concentration [22]. In Fig. 2, the L–H plot and constants are presented for Remazol Black B.

The decrease in photocatalytic decolourization rate at high concentrations can also be explained by the competitive absorption of dye and TiO_2 for near-UV light. Hence this effect reduces the photoactivity of TiO_2 for the formation of $OH^{\bullet}$ (radicals. This behaviour clearly reveals that at high dye concentrations, the reaction rate is limited by the concentration of oxidants, namely hydroxyl radicals produced on TiO_2 surface.

Change in absorbance at 254 nm throughout the photocatalytic oxidation representing the total aromatic content of the samples is illustrated in Fig. 3 for the 25–150 mg/l concentration range of the azo dye.

For up to 75 mg/l no decrease was observed within the first reaction hour; however, after 1 h when decolourization was almost complete, the reduction in $UV_{254\ nm}$ started. As can be seen from Fig. 4, COD removal as a function of the reaction time exhibited a similar trend to the absorbance removal at 254 nm.

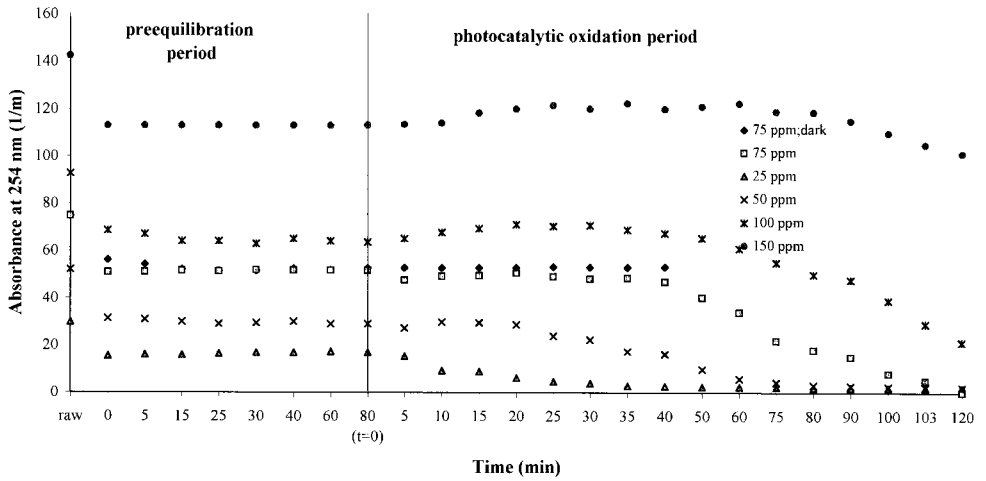

Fig. 3. Removal of absorbance at 254 nm by photocatalytic oxidation of Remazol Black B at various initial concentrations.

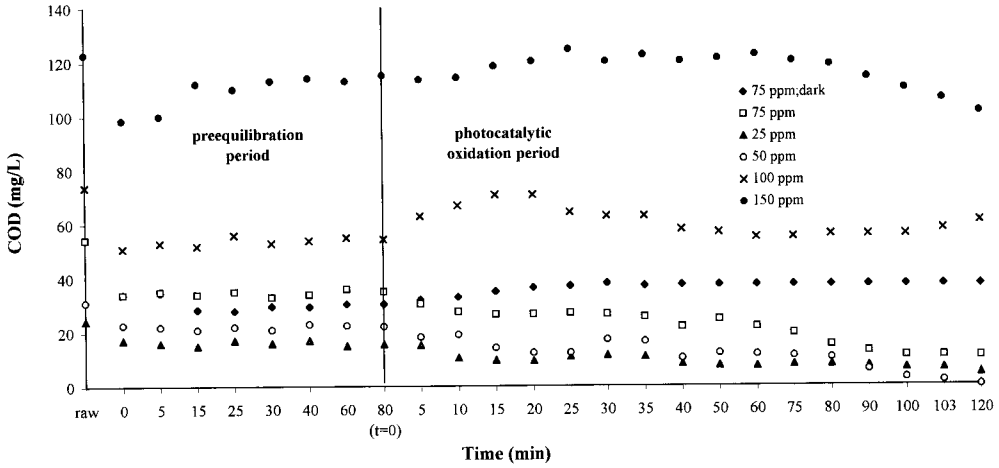

Fig. 4. Removal of COD by photocatalytic oxidation of Remazol Black B at various initial concentrations.

For both parameters no significant reduction was achieved for 150 mg/l dye concentration. These observations support the above suggested idea about the competition between TiO_2 sites and dye molecules for light absorption.

In the case of Remazol Turquoise Blue G 133, the decrease in colour (absorbance at 626 nm), 254 nm absorbance and COD as a function of photocatalytic treatment time are given in Figs. 5–7, respectively.

A significantly different reaction profile was observed for photocatalytic degradation of the copper complex dye for which colour removal is mainly due to dark adsorption on the photocatalyst surface during the preequilibration period. The initial photocatalytic decolourization rate after this period was only 0.38 1/(m.min). Thus for the copper complex dye degradation seems to be independent of initial dye concentration. After 120 min, 81% of colour and 68% of original COD were removed by preequilibration adsorption plus photooxidative degradation. The overall colour and COD removal data for 75 mg/l Remazol Turquoise Blue G133 and Remazol

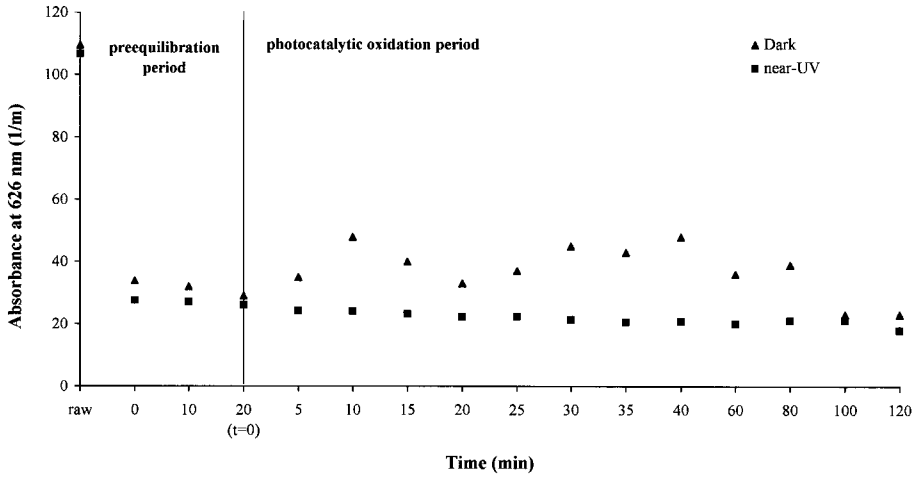

Fig. 5. Photocatalytic decolourization of 75 mg/l Remazol Turquoise Blue G 133.

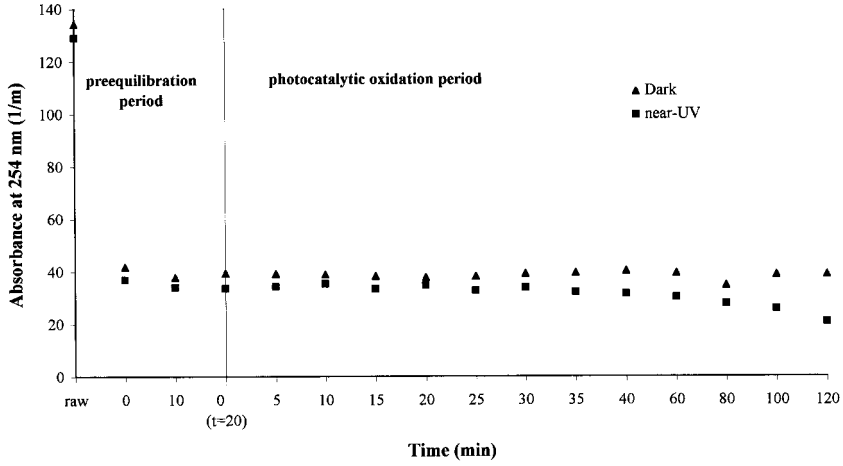

Fig. 6. Removal of absorbance at 254 nm by photocatalytic oxidation of 75 mg/l Remazol Turquoise Blue G 133.

Black B by photocatalytic oxidation are provided in Table 3.

It has to be pointed out that because of the strong adsorption of the copper complex dye on TiO_2, dye content in the bulk phase was not representative of the system. Therefore, it seemed that photocatalytic degradation was not responsible for the removal of the dye. Consequently, examination of decolourization kinetics at different initial dye concentrations was not applied to Remazol Turquoise Blue G 133.

Results of the photodegradation tests are in contrast to the general opinion that the efficiency of oxidation strongly depends upon the adsorptive properties of the samples [12] since for the more strongly adsorbed copper complex dye a slight photodegradation took place whereas the azo dye with weak adsorption properties photocatalytically degraded very quickly. This discrepancy may be related to differences in molecular structures and hence stability of the dyes.

3.4. Fenton and photo-Fenton reactions

The results of Fenton, photo-Fenton and control experiments of Remazol Black B dye at 75

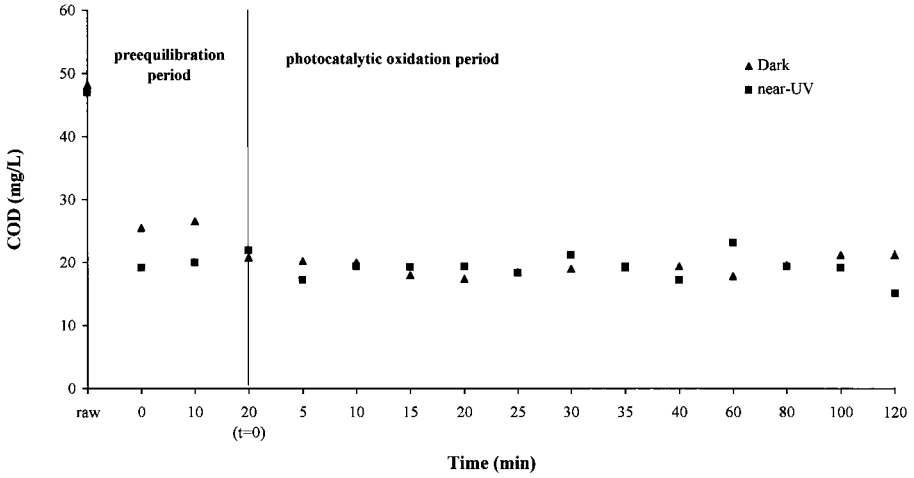

Fig. 7. Removal of COD by photocatalytic oxidation of 75 mg/l Remazol Turquoise Blue G 133.

Table 3
Overall colour and COD removal percentages for 75 mg/l Remazol Turquoise Blue G133 and Remazol Black B by photocatalytic oxidation

Dye	COD (%)[a]	Colour (%)[a]
Turquoise Blue G133	67.58 (53.21)	80.91 (72.32)
Black B	80.36 (35.43)	100.00 (27.41)

[a] Removal due to initial dark adsorption in parentheses.

mg/l concentration are shown in Fig. 8. The dark control test with H_2O_2 added at the same dose as in the Fenton and photo-Fenton experiments clearly revealed that dye degradation was caused by radical-initiated oxidation in other words the aggressive and nonselective attack by $OH^{\bullet}$ radicals is necessary for dye decolourization. The selected dose of Fenton's reagent was sufficient for almost instantaneous colour and COD removal, which implies that applied oxidants were available at excess concentrations causing no limitation of the reaction. As expected, initial decolourization rate [$r_i = 140.97$ 1/(m.min)] is increased [$r_i = 185.28$ 1/(m.min)] for the photo-Fenton process due to reproduction of catalyst ferrous ions which continue to react with excess H_2O_2 in the medium. Additional $OH^{\bullet}$ radicals are produced as follows [23–25]:

$$Fe^{3+} + h\nu \rightarrow Fe^{2+} \quad \text{(photoreduction)} \tag{1}$$

$$Fe(OH)^{2+} + h\nu \rightarrow Fe^{2+} + OH^{\bullet} \tag{2}$$

Moreover, photolysis of Fe(III)-dye chelates which are formed during photooxidation can produce organic radicals resulting in an enhanced rate of destruction of dye molecules [26];

$$Fe(III) - dye + h\nu \rightarrow Fe^{2+} + dye^{\bullet} \tag{3}$$

With 99% (two orders of magnitude) colour removal in only 3 min treatment time the Fenton's decolourization was 20 times faster than TiO_2-mediated photocatalytic oxidation. Fig. 9 depicts COD removal for 75 mg/l Remazol Black B by the Fenton and photo-Fenton reactions. No COD removal was observed for the dark control run in the absence of ferrous catalyst. The difference between Fenton and photo-Fenton reactions for COD reduction of the azo dye was insignificant.

Colour and COD removal for 75 mg/l Remazol Turquoise Blue G 133 by Fenton and photo-Fenton oxidation are presented in Figs. 10 and 11, respectively. Here again the homogenous initial decolourization rate [$r_i = 0.8875$ 1/(m.min) for Fenton, $r_i = 1.2112$ 1/(m.min) for photo-Fenton] was two times faster than the photocatalyzed

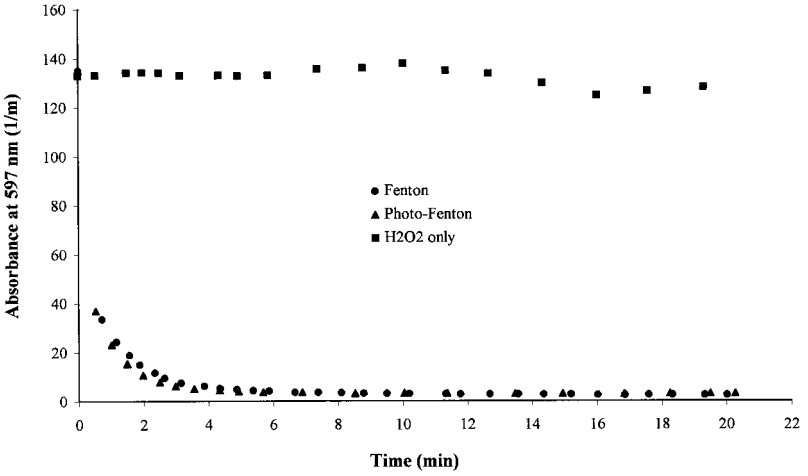

Fig. 8. Decolourization of 75 mg/l Remazol Black B by Fenton and photo-Fenton reactions.

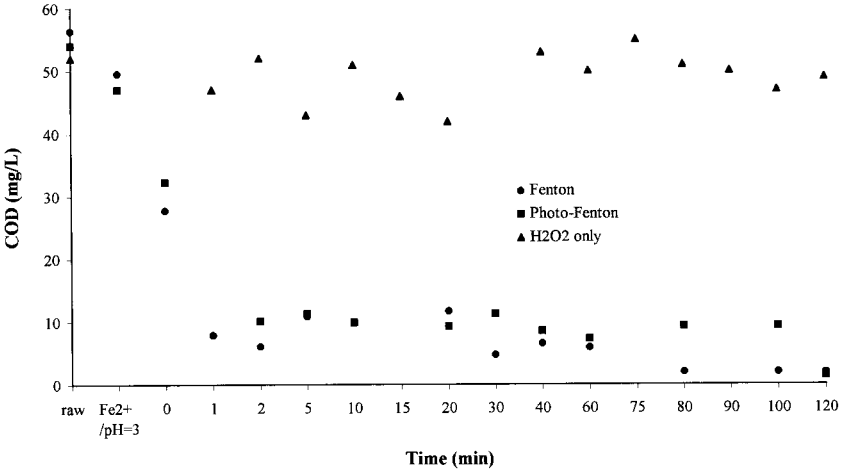

Fig. 9. COD removal of 75 mg/l Remazol Black B by Fenton and photo-Fenton reactions.

oxidation of the copper phthalocyanine dye following an overall zeroth order kinetics. The overall COD removals are 63% for dark and 68% for light-induced Fenton reactions respectively. Eighteen per cent of it was removed on MnO_2 used for H_2O_2 destruction. An average initial 17% reduction of COD with Fe^{2+} ions was probably the coagulating effect of iron salt for Remazol Turquoise Blue G 133.

3.5. Fenton-like and photo-Fenton-like reactions

Decolourization of 75 mg/l Remazol Black B by the Fenton-like reactions are presented in Fig. 12. In this case, the effect of light was more significant, whose introduction gave a nearly fivefold acceleration of the initial decolourization rate. This difference was expected since dark Fenton-like oxidation continues via $HO_2^{\bullet}$ radicals that are

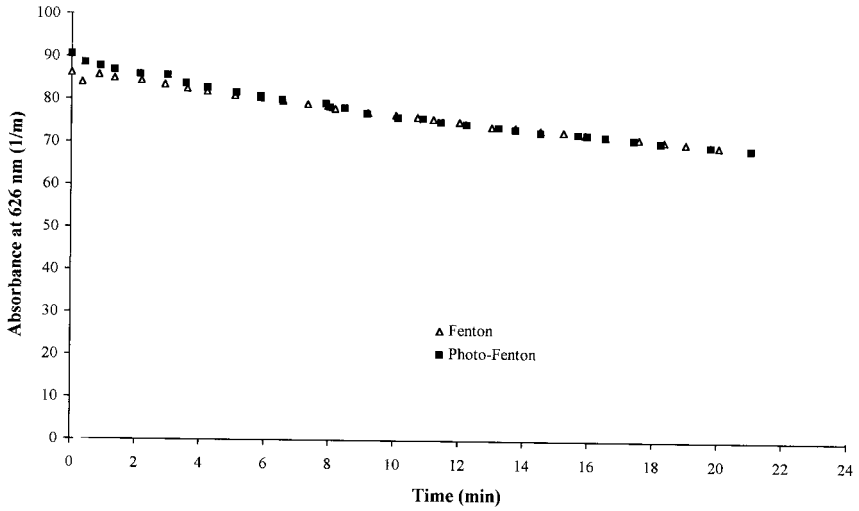

Fig. 10. Decolourization of 75 mg/l Remazol Turquoise Blue G 133 by Fenton and photo-Fenton reactions.

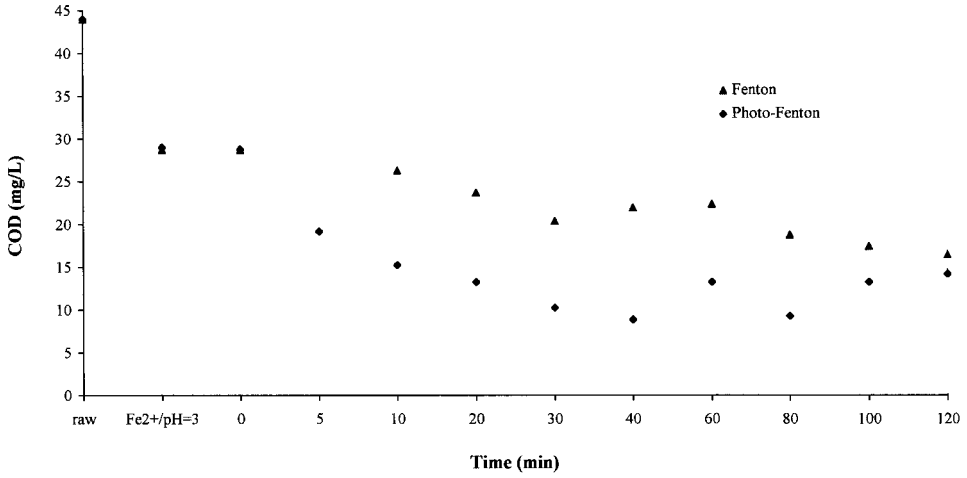

Fig. 11. COD removal of 75 mg/l Remazol Turquoise Blue G 133 by Fenton and photo-Fenton reactions.

known to react considerably slower than the $OH^{\bullet}$ radicals [23,27]. From the results of homogenous decolourization rates one may conclude that due to the narrow absorption band of the black light lamp only limited light quanta are available for the photoreduction of ferric iron to ferrous iron and hence direct Fenton's oxidation plays a major role in degradation of the dye molecules. Thus, almost no difference between the dark and photo-Fenton's oxidations rates could be observed.

COD reduction for the Fenton-like runs emphasized that the concentration-dependent decrease proceeded so fast in the case of Remazol Black B that no remarkable change in COD value occurred after the first few minutes of advanced oxidation reaction (Fig. 13). Sixty-three and 66% COD reduction for Fenton-like and photo-Fenton-like oxidations was obtained respectively. On the other hand, initially 32–29% reduction in COD was obtained for the azo dye as a result of

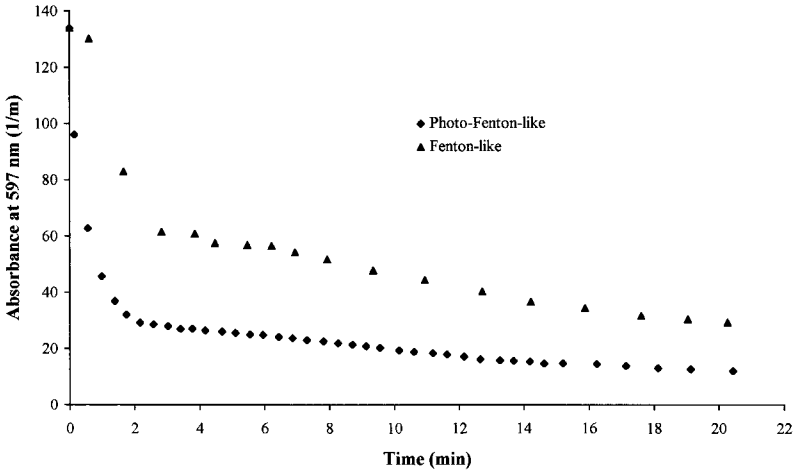

Fig. 12. Decolourization of 75 mg/l Remazol Black B by Fenton-like and photo-Fenton-like reactions.

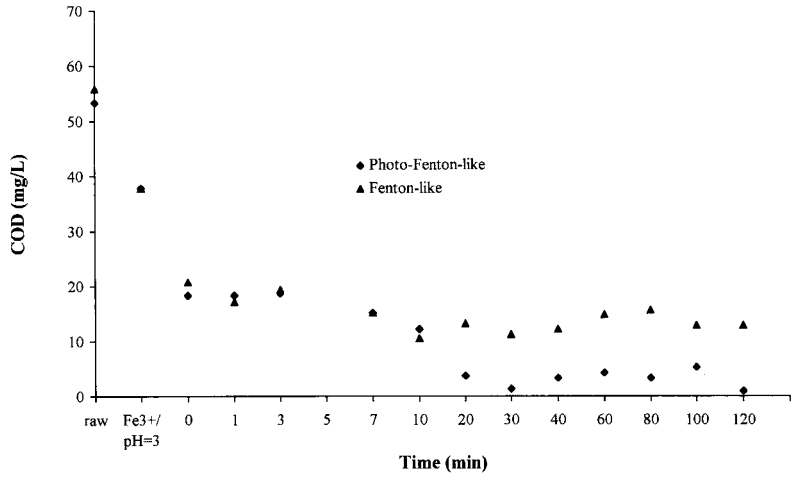

Fig. 13. COD removal of 75 mg/l Remazol Black B by Fenton-like and photo-Fenton-like reactions.

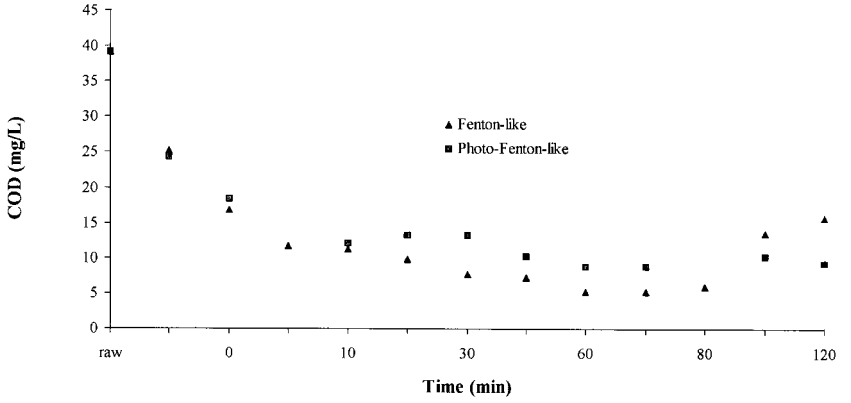

Fig. 14. COD removal of 75 mg/l Remazol Turquoise Blue G 133 by Fenton-like and photo-Fenton-like reactions.

ferric iron chemical coagulation [28] as observed by substantial floc formation during the reaction. Initial 57% (Fenton-like) and 53% (photo-Fenton-like) COD removal at $t = 0$ min for the copper complex dye was due to the coagulating effect of ferric iron plus adsorption on MnO_2. Overall COD reduction after two hours treatment were 60% for dark and 76% for simultaneously light-assisted oxidations (Fig. 14). Changes in absorbance during dark and photo-Fenton-like reactions could not be measured correctly due to formation of Fe^{3+} flocs. Tables 4 and 5 summarize initial

Table 4
Initial decolourization rates (r_i), overall TOC and COD removal percentages for degradation of 75 mg/l Remazol Black B by various AOP's

Process	TiO_2/near-UV	Fenton	Fenton/near-UV	Fenton-like	Fenton-like/near-UV
r_i (1/(m.min))	4.29	140.97	185.28	26.82	125.22
TOC (%)[a]	70.00	51.00	nd[c]	nd	86.00
COD (%)[b]	80.36	96.60	97.50	77.00	98.20

[a] 52% removal by Fe^{3+} coagulation, 23% by initial dark adsorption on TiO_2 surface.
[b] 31% removal by Fe^{3+} coagulation, 37% by initial dark adsorption on TiO_2 surface.
[c] Not determined.

Table 5
Initial decolourization rates and overall COD removals for degradation of 75 mg/l Remazol Turquoise Blue G133 by various AOP's

Process	TiO_2/near-UV	Fenton	Fenton/near-UV	Fenton-like	Fenton-like/near-UV
r_i (1/(m.min))	0.38	0.8875	1.2124	–	–
COD (%)	67.60 (53.20)[a]	62.70 (16.00)[b]	67.70 (16.70)[b]	60.10 (35.70)[c]	76.30 (37.70)[c]

[a] Initial dark adsorption on TiO_2.
[b] Coagulation by Fe^{2+}.
[c] Coagulation by Fe^{3+}.

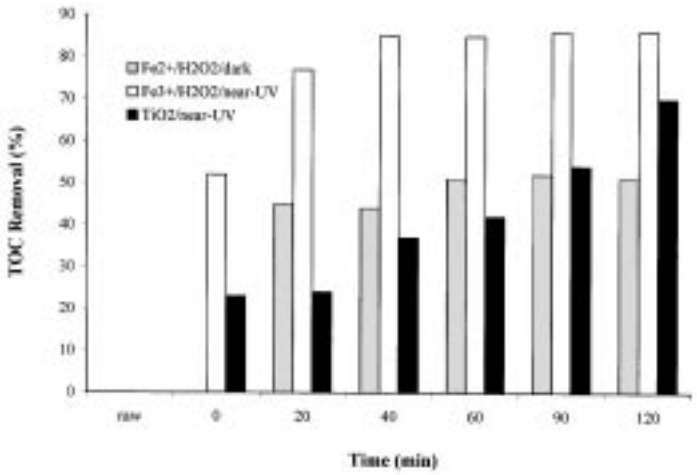

Fig. 15. TOC removal during advanced oxidation of 75 mg/l Remazol Black B by dark-Fenton, photo-Fenton-like and TiO_2-mediated photocatalytic reactions.

decolourization rates, overall TOC and COD removals for the degradation of 75 mg/l Remazol Black B and Remazol Turquoise Blue G133 by various AOPs.

3.6. Comparison of TOC removal for the advanced oxidation systems

The results for TOC removal of Remazol Black B by photo-Fenton-like, Fenton and TiO_2/near-UV are compared in Fig. 15. The figure indicates that 100, 48 and 77% of the overall TOC removal was due to mineralization via Fenton, photo-Fenton-like and TiO_2/near-UV oxidations respectively.

4. Conclusions

For both Remazol dyes, adsorption on TiO_2 was found favourable by the Langmuir approach ($K_L = 0.42$ mg/l for Remazol Black B and 3.42 mg/l for Remazol Turquoise Blue G 133). All investigated AOPs are capable of completely decolourizing the azo dye Remazol Black B within feasible reaction times ranging from a few minutes to 1 h by homogenous and heterogenous advanced oxidation systems respectively. Initial decolourization rate by homogenous advanced oxidation was 6–44 times faster than by the TiO_2-mediated photocatalytic reaction for the azo dye. For Remazol Black B initial photocatalytic decolourization rates could be fitted to the empirical Langmuir-Hinshelwood equation [$k_{L-H} = 5.097$ 1/(m.min); $K_{ads} = 0.153$ l/mg) up to 100 mg/l initial dye concentration preequilibrated prior to the introduction of light. Photocatalytic degradation of this azo dye was limited at higher doses by factors such as insufficient $OH^{\bullet}$ production, due to competition between solute and formed radicals for active sites on the photocatalyst surface. As a result, decrease in COD and $UV_{254\ nm}$ appeared to be significant only after total decolourization. Decreasing order of initial decolourization rates for different AOPs was found as photo-Fenton > dark-Fenton > photo-Fenton-like > Fenton-like > TiO_2-mediated photocatalytic oxidation. For 75 mg/l Remazol Black B, the photo-Fenton-like oxidation system resulted in an overall 86% TOC and 98% COD removal within 2 h treatment. On the other hand, the copper phthalocyanine dye showed negligible degradation by all AOPs; dye treatment with coagulants/adsorbents would be more effective and hence advisory. Homogenous oxidation of the all dyestuffs was fairly enhanced by near-UV irradiation. Introduction of near-UV light for the Fenton/Fenton-like processes could only slightly improve the water quality parameters and decolourization rates, but at the expense of a more complex and costly operation. Currently, the impact of various dyebath components such as salts, alkali, sequestering agents and surfactants on the oxidative efficiency and reaction kinetics of homogenous and heterogenous AOPs is under investigation.

Acknowledgements

The authors acknowledge the support of Bogaziçi University Research Fund of this project (no. 98 Y03). The supply of gift sample Remazol dyes by Dystar (Hoechst Corp., Turkey) is greatly appreciated.

References

[1] Grau P. Textile industry wastewaters treatment. Wat Sci Technol 1991;24:97.
[2] Reife A. Dyes, environmental chemistry. Kirk-Othmer Encyclopedia of Chemical Technology. 4th ed. p.753. Washington: John Wiley & Sons, Inc., 1993.
[3] Pagga U, Braun D. The degradation of dyestuffs: Part II behaviour of dyestuffs in aerobic biodegradation tests. Chemosphere 1986;15:479.
[4] Wu J, Eiteman MA, Law SE. Evaluation of membrane filtration and ozonation processes for treatment of reactive-dye wastewater. J Environ Eng 1998;124:272.
[5] Bahorsky MS. Textiles. Wat Environ Res 1997;69:658.
[6] Balcioglu IA, Arslan I. Treatment of textile wastewater by heterogenous photocatalytic oxidation processes. Environ Technol 1997;18:1053.
[7] Legrini O, Oliveros E, Braun AM. Photochemical processes for water treatment. Chem Rev 1993;93:671.
[8] Marechal ML, Slokar YM, Taufer T. Decoloration of chlorotriazine reactive azo dyes with H_2O_2/UV. Dyes and Pigments 1997;33:281.
[9] Ince NH, Stefan MI, Bolton JR. UV/H_2O_2 degradation and toxicity reduction of textile azo dyes: Remazol Black-B, a case study. J Adv Oxid Technol 1997;2:442.

[10] Kang SF, Chang HM. Coagulation of textile secondary effluents with Fenton's reagent. Wat Sci Technol 1997;36:215.
[11] Kuo WG. Decolorizing dye wastewater with Fenton's reagent. Wat Res 1992;26:881.
[12] Zhang F, Zhao J, Shen T, Hidaka H, Pelizetti E, Serpone N. TiO_2-assisted photodegradation of dye pollutants II. Adsorption and degradation kinetics of eosin in TiO_2 dispersions under visible light irradiation. Appl Cat B: Environmental 1998;15:147.
[13] Tang WZ, Zhang Z, An H, Quintana MO, Torres DF. TiO_2/UV photodegradation of azo dyes in aqueous solutions. Environ Technol 1997;18:1.
[14] Morrison C, Bandara J, Kiwi J. Sunlight induced decolouration/degradation of non-biodegradable Orange II dye by advanced oxidation technologies in homogenous and heterogenous media. J Adv Oxid Technol 1996;2:160.
[15] Vinodgopal K, Bedja I, Hotchandani S, Kamat PV. A photocatalytic approach for the reductive decolourization of textile azo dyes in colloidal semiconductor suspensions, Langmuir 1994;10:1767 [reprint].
[16] Hustert K, Zepp RG. Photocatalytic degradation of selected azo dyes. Chemosphere 1992;24:335.
[17] Reeves P, Ohlhausen R, Sloan D, Pamplin K, Scoggins T, Clark C, Hutchinson B, Green D. Photocatalytic destruction of organic dyes in aqueous TiO_2 suspensions using concentrated simulated and natural solar energy. Solar Energy 1992;6:413.
[18] Shore J. Cellulose dyeing. Oxford: Alden Press, 1995 [Society of Dyes and Colorists].
[19] Balcioglu IA, Arslan I. Application of photocatalytic oxidation treatment to pretreated and raw effluents from Kraft bleaching process and textile industry. Environ Pollut 1998;103:261.
[20] Vermeulen T, Le Van MD, Hiester NK, Klein G. Adsorption ion exchange. In: Perry RH, Green D, editors. Perry's chemical engineers' handbook. New York: McGraw Hill, 1984.
[21] Juang RS, Wu FC, Tseng RL. The ability of activated clay for the adsorption of dyes from aqueous solutions. Environ Technol 1997;18:525.
[22] Matthews RW. Kinetics of photocatalytic oxidation of organic solutes over titanium dioxide. J Catal 1988;111:264.
[23] Balzani VC, Carasitti V. Photochemistry of coordination compounds. New York: Academic Press, 1970. p. 172.
[24] Walling C. Fenton's reagent revisited. Accounts of Chemical Research 1975;8:125.
[25] Ruppert G, Bauer R, Heisler G. The photo-Fenton reaction — an effective photochemical wastewater treatment process. J Photochem Photobiol A: Chem 1993;73:75.
[26] Safarzadeh-Amiri A, Bolton RJ, Cater SR. The use of iron in advanced oxidation processes. J Adv Oxid Technol 1996;1:18.
[27] Pignatello JJ. Dark and photoassisted Fe^{3+}-catalyzed degradation of chlorophenoxy herbicides by hydrogene peroxide. Envi Sci Technol 1992;26:941.
[28] Walling C, Kato S. The oxidation of alcohols by Fenton's reagent: the effect of copper ion. J Am Chem Soc 1971;93:4275.